Pergamon

Comp. Maths Math. Phys., Vol. 35, No. 8, pp. 949–957, 1995

0965–5425/95 $24.00 + .00

0965-5425(95)00116-6

THE USE OF MOVING ADAPTIVE GRIDS IN ALGORITHMS WITH COMPACT APPROXIMATIONS†

D. Zh. GAN'ZHA, I. F. MUZAFAROV and
S. V. UTYUZHNIKOV

Moscow

(*Received* 17 *December* 1994)

For the finite difference method with compact approximations, a procedure for using moving curvilinear grids that are adaptive to the solution is described. In analysing the method, attention is mainly paid to the geometric conservation laws. The efficiency of the approach and greater effectiveness of the use of adaptive grids as compared with uniform grids are demonstrated using numerical examples.

1. INTRODUCTION

The calculation grids used in the numerical simulation of the flows of a compressible gas should, on the one hand, take into account the specific features of the phenomenon under investigation and, on the other, be consistent with the numerical algorithm used to ensure sufficient accuracy.

Thus, when solving problems on the flows in the stratified atmosphere of the earth, the domain of the phenomenon investigated can change considerably in size and in its position in space. The calculation domain must, therefore, either be large enough to allow for all possible variations right from the start (placing great demands on the computer capability) or change during the computation.

The use of algorithms with compact approximations makes it possible to achieve high computational accuracy on a compact pattern, even with a comparatively small number of grid nodes. However, if the solution inside the domain has small subdomains with sharp gradients, the solution obtained with higher-order schemes on ordinary grids and with realistic spatial steps might be even less accurate than with ordinary difference schemes of a low order of approximation. The use of adaptive grids smoothes the solution in the new transformed coordinates and allows higher-order schemes actually to achieve a high order of accuracy.

The family of compact difference schemes proposed in [1] is intended for equations represented in conservative form. The purpose of the present paper is to construct a finite difference method using compact approximations and moving adaptive curvilinear grids.

2. THE SYSTEM OF EQUATIONS. THE GEOMETRIC CONSERVATION LAWS

We will write the system of governing equations in a Cartesian system of coordinates $\{t, x^i\}$ in conservative form:

† *Zh. Vychisl. Mat. Mat. Fiz.* Vol. 35, No. 8, pp. 1184–1194, 1995.

$$\frac{\partial}{\partial t} q + \frac{\partial}{\partial x^j} ie^j = 0. \tag{2.1}$$

Here and below summation is taken over repeated indices. We transfer to the arbitrary system of coordinates $\{t, x^j\} \to \{\tau, \xi^j\}$:

$$\xi^j = \xi^j (t, x^i), \quad \tau = t.$$

The system of equations (2.1) can be written in strictly conservative form in the new variables:

$$\frac{\partial}{\partial \tau} \frac{q}{J} + \frac{\partial}{\partial \xi^j} (\hat{\xi}^j_t q + \hat{\xi}^j_{x^i} e^i) = 0. \tag{2.2}$$

Here

$$\hat{\xi}^j_t = \frac{1}{J} \frac{\partial \xi^j}{\partial t}, \quad \hat{\xi}^j_{x^i} = \frac{1}{J} \frac{\partial \xi^j}{\partial x^i}, \quad J = \det \| \xi^j_{x^i} \|.$$

We will now write a two-layer one-parameter difference approximation:

$$\Delta q^n = \tau \frac{\partial}{\partial \tau} q^n + \theta \tau \frac{\partial}{\partial \tau} \Delta q^n + O(\tau^3 + \tau^2 (0.5 - \theta)) = \tau \frac{\partial}{\partial \tau} \bar{q}. \tag{2.3}$$

Here θ is a certain parameter, τ is the time step. In addition, we have used the notation

$$\bar{f} = (1 - \theta) f^n + \theta f^{n+1}, \quad \Delta q^n = q^{n+1} - q^n.$$

Applying (2.3) to (2.2), we can write an approximation of Eq. (2.2) with respect to time:

$$\left\{ I + \theta \tau \frac{\partial}{\partial \xi^j} [\hat{\xi}^{j\,n+1}_t I + \hat{\xi}^{j\,n+1}_{x^i} E^{i\,n}] \right\} \Delta \left(\frac{q}{J} \right)^n = \tag{2.4}$$

$$= -\tau \frac{\partial}{\partial \xi^j} \left[\left(\frac{q}{J} \right)^n \bar{\hat{\xi}}^j_t + \left(\frac{e^i}{J} \right)^n \bar{\hat{\xi}}^j_{x^i} \right].$$

Here I is the identity matrix and $E^{i\,n} = \partial e^{i\,n} / \partial q^n$ is the Jacobian of the flow vector. If the equation is written with respect to "pure flow variables" Δq^n, we obtain

$$\left\{ \frac{1}{J^n} + \theta \tau \frac{\partial}{\partial \xi^j} [\hat{\xi}^{j\,n+1}_t I + \hat{\xi}^{j\,n+1}_{x^i} E^{i\,n}] \right\} \Delta q^n = -q^n \Delta \frac{1}{J^n} - \tau \frac{\partial}{\partial \xi^j} [q^n \bar{\hat{\xi}}^j_t + e^{i\,n} \bar{\hat{\xi}}^j_{x^i}]. \tag{2.5}$$

To solve (2.4) or (2.5), we need to choose a difference scheme to approximate the spatial derivatives and a method of inverting the operator on the left-hand side.

We can conditionally divide the variables into flow (q, e^i) and geometric variables (J, $\hat{x}^j_t$, $\hat{x}^j_{x^i}$). However, the governing equation (2.2) is written in new variables (q/J, . . .) obtained by combining the old ones. This will lead to numerical errors, even if the solution is known exactly. For, the geometric variables (J, $\hat{\xi}^j_t$, $\hat{\xi}^j_{x^i}$) are subject to their own identities (geometric conservation laws [2]), which are easy to obtain from the system of differential equations (2.2) by putting q, e^i = const.

$$\frac{\partial}{\partial \tau} \frac{1}{J} + \frac{\partial}{\partial \xi^j} \hat{\xi}^j_t = 0, \tag{2.6}$$

$$\frac{\partial}{\partial \xi^j} \hat{\xi}^j_{x^i} = 0, \quad i = 1, 2, 3. \tag{2.7}$$

These relations are satisfied exactly in the differential case. However, when the equations are discretized the extent to which they are satisfied depends on the method used to compute the geometric variables.

Relation (2.6) is called the volume conservation law (VCL). The VCL must be taken into account if the system of coordinates is a moving one. The second relation means that the operations of differentiation for the calculation of Eqs (2.2) and the computation of the metric coefficients $\hat{\xi}^j_{x^i}$ are commutative. For example, in the two-dimensional case (2.7) takes the form

$$\frac{\partial}{\partial \xi} x_\eta = \frac{\partial}{\partial \eta} x_\xi, \quad \frac{\partial}{\partial \xi} y_\eta = \frac{\partial}{\partial \eta} y_\xi.$$

3. SATISFYING THE VOLUME CONSERVATION CONDITION

The difference analogue of the VCL might not be satisfied in the case of a moving system of coordinates. One way of satisfying the condition of the VCL is to find the Jacobian of the transformation to the new system of coordinates by solving Eq. (2.6) directly by the same method as the "basic" equation (2.2), instead of using the formula $J = \det \| \xi^j_x \|$.

For Eq. (2.4) this leads to the relation

$$\left\{ I + \theta\tau \frac{\partial}{\partial \xi^j} \xi^{j\,n+1}_t \right\} \Delta \frac{1}{J^n} = -\tau \frac{\partial}{\partial \xi^j} \left(\frac{J^n}{J} \bar{\xi}^j_t \right). \tag{3.1}$$

In the case of Eq. (2.5) we have

$$\left(\Delta \frac{1}{J^n} \right) = -\tau \frac{\partial}{\partial \xi^j} [\bar{\xi}^j_t]. \tag{3.2}$$

Thus, the solution of Eq. (2.2) will reduce to the solution of the pairs of equations (3.1), (2.4) or (3.2), (2.5).

Although there is some loss of conservativeness with respect to time on changing from the variable J/q to q, the numerical calculation of Eqs (3.2) and (2.5) is preferable to that of Eqs (3.1) and (2.4). The following arguments can be used to support this view:

solving the VCL is considerably simpler with (3.2) than with (3.1), by virtue of the fact that it is explicit in form;

in (2.5) the variation with respect to time of the variable $1/J$ is allowed for on the right-hand side of Eq. (2.5), that is, explicitly; this is consistent with the fact that when the solution q^{n+1} is calculated on the $(n+1)$-th time layer it is assumed that the grid $\{x^{i\,n+1}\}$ is already known.

In the numerical implementation of Eqs (3.1) and (3.2), the spatial derivatives must be approximated with the same difference formulae as in Eqs (2.4) and (2.5). If the difference schemes are asymmetric (for instance, if they allow for the characteristic properties of the hyperbolic part of the system of equations), this condition is difficult to satisfy. In the practical implementation of (3.1) and (3.2) in the difference schemes the asymmetry parameter was assumed to be zero. There also remains some arbitrariness in the method of computing the metric coefficients $\hat{\xi}^j_t$. A numerical experiment showed that negligibly small numerical errors arose when calculating a solution that was constant in time and space by formulae (3.1), (2.4) or (3.2), (2.5). However, the calculation of flows which were unsteady with respect to time or space displayed errors. These arose if the boundaries of the cells of the calculation grid did not move in parallel-translational fashion. In that case the errors increased as the rate of flow increased, that is, as the importance of asymmetry of the difference scheme increased. If the rates of flow and the rate at which the nodes of the difference grid move are comparable with the speed of sound, the errors, while smaller than the solution itself, are comparable in order of magnitude.

We will now examine whether there are better ways of computing the geometric variables.

4. INTERPRETING THE GEOMETRIC VARIABLES IN THE FINITE DIFFERENCE METHOD (FDM) AS VARIABLES OF THE FINITE VOLUME METHOD (FVM)

The volume conservation law is a necessary, but not sufficient condition for conservation of a constant solution. An example of a rotating non-inertial system of coordinates is given in [3], where the calculation of the equation for the VCL can lead to a non-physical variation in time of $1/J$ and, therefore, to errors in calculating the flow variables.

The following method of calculating the metric coefficients, based on the FVM of [3], is interesting.

In the FVM, for each elementary cell the volume V and the vectors of the normal S^{ξ^j} to the cell boundaries, equal in modulus to the area of that boundary, are calculated. We will introduce the variable V_s, denoting the change of volume V (allowing for sign) as a result of the boundary of the cell S moving for a time $\Delta t = t_2 - t_1$:

$$V(t_2) - V(t_1) = \sum_{\text{cell}} V_s.$$

The symbol $\sum_{\text{cell}}$ denotes summation over all the cell faces.

In the FDM, consider a cell of twice the size in every direction, with centre at the given point. We can then compare the geometric variables of the FDM and FVM:

$$\mathbf{r} = \mathbf{r}(\xi, \eta, \zeta, \tau), \quad t = \tau, \quad \frac{\nabla\xi}{J} = \frac{1}{J}(\xi_x, \xi_y, \xi_z)^T = \mathbf{r}_\eta \times \mathbf{r}_\zeta = \mathbf{S}^\xi, \tag{4.1a}$$

$$\frac{\xi_t}{J} = -\mathbf{S}^\xi \cdot \mathbf{r}_\tau, \quad J = \frac{1}{V}. \tag{4.1b}$$

Here r_τ is the velocity of the node, $\mathbf{S}^\xi$ is the normal to the boundary of twice the size and V is the volume of the double cell. In the new variables, relations (2.6) and (2.7) can be written in the form

$$V_\tau = (\mathbf{S}^\xi \cdot \mathbf{r}_\tau)_\xi + (\mathbf{S}^\eta \cdot \mathbf{r}_\tau)_\eta + (\mathbf{S}^\zeta \cdot \mathbf{r}_\tau)_\zeta, \tag{4.2}$$

$$(\mathbf{S}^\xi)_\xi + (\mathbf{S}^\eta)_\eta + (\mathbf{S}^\zeta)_\zeta = \mathbf{0}. \tag{4.3}$$

We will represent the variable $\hat{\xi}_i$ as follows:

$$\hat{\xi}_i = \frac{\xi}{J} = -\frac{1}{\Delta t}\int_{t_1}^{t_2} \mathbf{S}^\xi \cdot \mathbf{r}_\tau dt = -\frac{V_s^\xi}{\Delta t}. \tag{4.4}$$

In (4.4) the variable $\hat{\xi}_i$ contains all the information on how the cell moves: the distance, the rotation and the deformation. By contrast, (4.1) is simply the product of the area by the velocity and represents parallel translation only.

In this approach, the metric time coefficients $\hat{\xi}_i^j$ are defined in such a way that the VCL condition is satisfied and the variable $1/J$ corresponds to the geometry of the problem $J = \|\xi_x^j\|$.

This approach operates with finite-difference cells of twice the size. If symmetric difference schemes are used (such as central difference schemes), the VCL (4.2) will be satisfied on a cell of twice the size. Thus, the original calculation grid separates into two grids with no nodes in common, with cells of twice the size, in each of which the VCL (4.2) is satisfied. Experience has shown that this approach can be successfully used to calculate the flows on moving grids which are uniform at each instant of time, even using asymmetric differences. These grids arose from the specific features of the problems to be solved: unsteady flows in a stratified atmosphere which describe the rising of a large thermal [4] (the domain of the physical phenomenon moves in space and its dimensions change). In the case of curvilinear moving grids with asymmetric difference schemes, this approach gives rise to considerable difficulties.

5. DIRECTED COMPACT DIFFERENCES AND ADAPTIVE MOVING GRIDS

The approaches described above preserve complete conservativeness of the representation of spatial derivatives. An alternative is the approach suggested in [5]. In numerical calculations, the equations are represented in CRCLF (Chain Rule Conservation Law Form), even in high-resolution schemes:

$$\frac{\partial}{\partial\tau} q + \xi_t^j \frac{\partial}{\partial\xi^j} q + \xi_x^k \frac{\partial}{\partial\xi^j} e^j = \mathbf{0}. \tag{5.1}$$

This equation can be obtained by transforming (2.2) identically, using (2.6) and (2.7).

In this equation all the flow variables are written in conservative form, and this governs the conservativeness properties in the numerical realization. At the same time, no additional relations for the geometric variables are required.

We could derive a discrete equation for the numerical solution (the analogue of (2.4) and (2.5)) starting from (5.1). However, if compact approximations [1] are used, it is important to write the left-hand side of the equation to be solved numerically in conservative form. In that case, inverting the operator on the left-hand side after factorizing it can reduce to three-point sweeps.

Thus transformations analogous to those carried out to obtain (5.1) will be performed with the discrete analogue of the differential equation (2.2), (2.5).

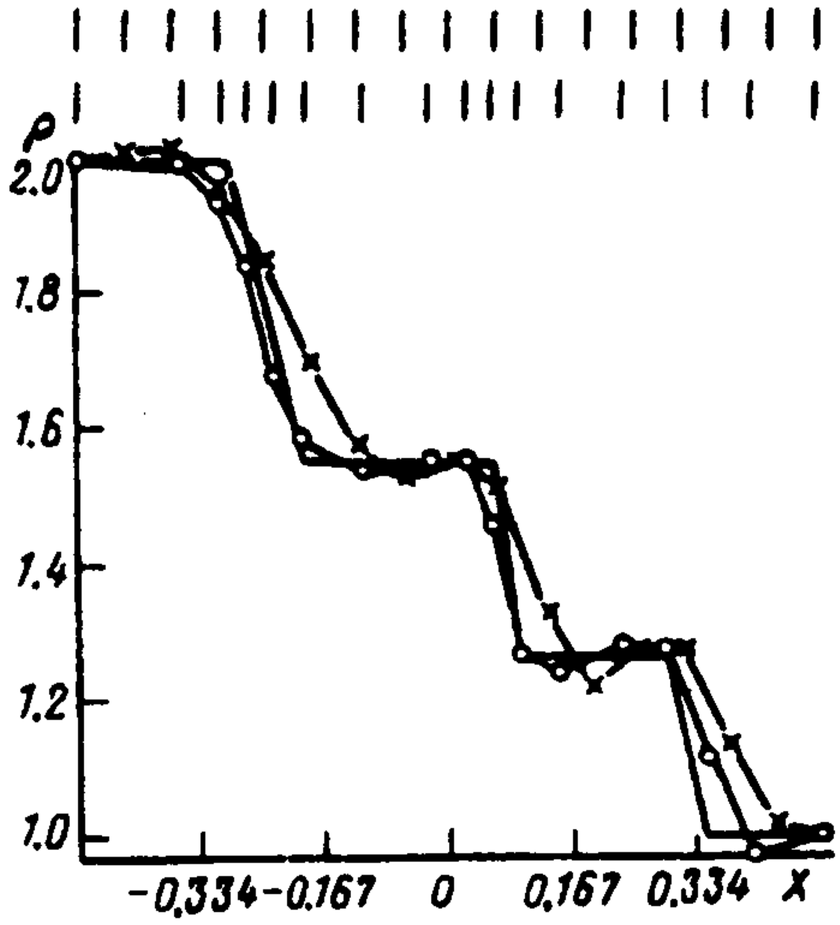

Fig. 1.

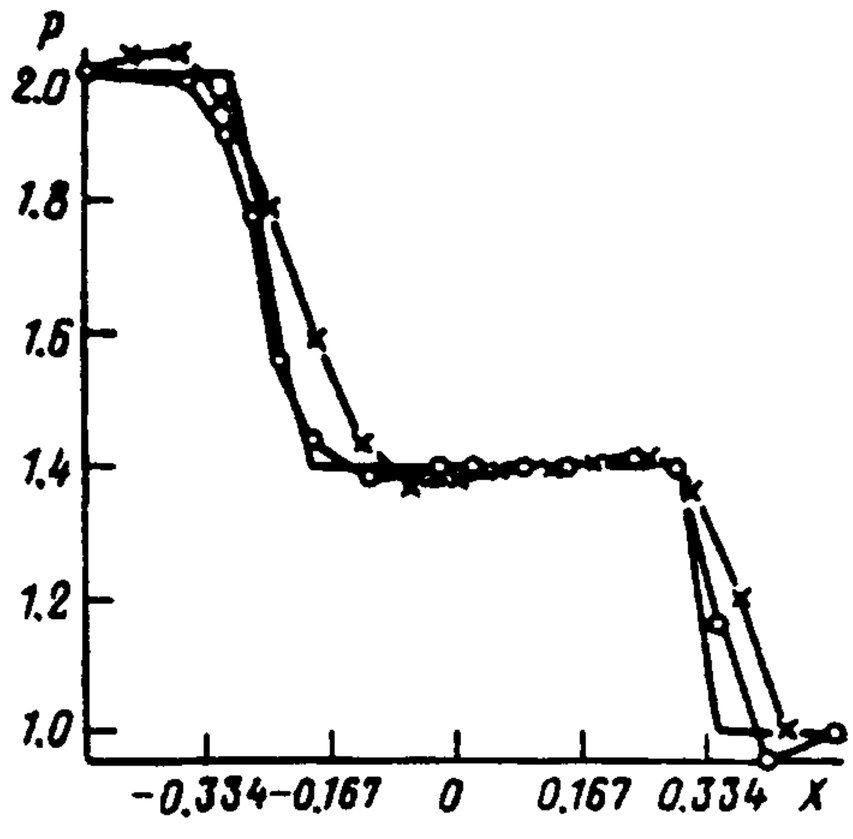

Fig. 2.

We will now consider Eq. (2.5), without transferring to the discrete representation of the derivatives with respect to space. We transform the right-hand side of (2.5), using (3.2) and (2.7):

$$-q^n\Delta\frac{1}{J^n}-\tau\frac{\partial}{\partial\xi^j}\left[q^n\bar{\xi}_t^j+e^n\bar{\xi}_x^j\right]=-\tau\bar{\xi}_t^j\frac{\partial}{\partial\xi^j}q^n-\tau\bar{\xi}_x^j\frac{\partial}{\partial\xi^j}e^n.$$

With the new right-hand side, Eq. (2.5) will take the form

$$\left\{\frac{1}{J^n}+\theta\tau\frac{\partial}{\partial\xi^j}\left[\hat{\xi}_t^{j\,n+1}I+\hat{\xi}_x^{j\,n+1}E^n\right]\right\}\Delta q^n=-\tau\bar{\xi}_t^j\frac{\partial}{\partial\xi^j}q^n-\tau\bar{\xi}_x^j\frac{\partial}{\partial\xi^j}e^n. \tag{5.2}$$

When the solution of this equation is a constant, we obtain the exact value of the required solution. For in that case the right-hand side of (5.2) is identically equal to zero and, therefore, $\Delta q^n = 0$.

As a result, relation (2.5) has been transformed so that automatic allowance is made for the conservation laws (2.6) and (2.7) on the right-hand side of the equation. Despite some loss of conservativeness, this approach can be used with success to calculate flows with large shocks by a high-resolution calculation, as was noted in [5] and has since been confirmed in numerical calculations. We note that in the approach proposed here, unlike [5], the metric coefficients are written in non-conservative form only on the right-hand side of the equation.

The numerical calculations did not reveal any additional sources of error. Thus, it can be concluded that the approach is suitable for numerical methods with compact approximations on moving adaptive grids.

The numerical examples given in the next section demonstrate, first, that the proposed method is suitable for solving the unsteady Euler (Navier–Stokes) equations on moving adaptive grids and, second, that it is effective.

6. EXAMPLES

To use the calculation grid on each time layer we solved an elliptic system of equations obtained by minimizing the functionals corresponding, after adaptation, to the solution, smoothness and orthogonality [6, 7].

Tolstykh's method of calculating the unsteady Euler (Navier–Stokes) equations using compact difference schemes is described in [4]. That method has been modified to allow for the technique described above.

As a test we solved the one-dimensional problem of decay of a discontinuity with the initial data (in dimensionless variables)

$$\rho(x),\ p(x)=\begin{cases}2 & \text{for } x<0.5,\\ 1 & \text{for } x\geq 0.5.\end{cases}$$

Fig. 3.

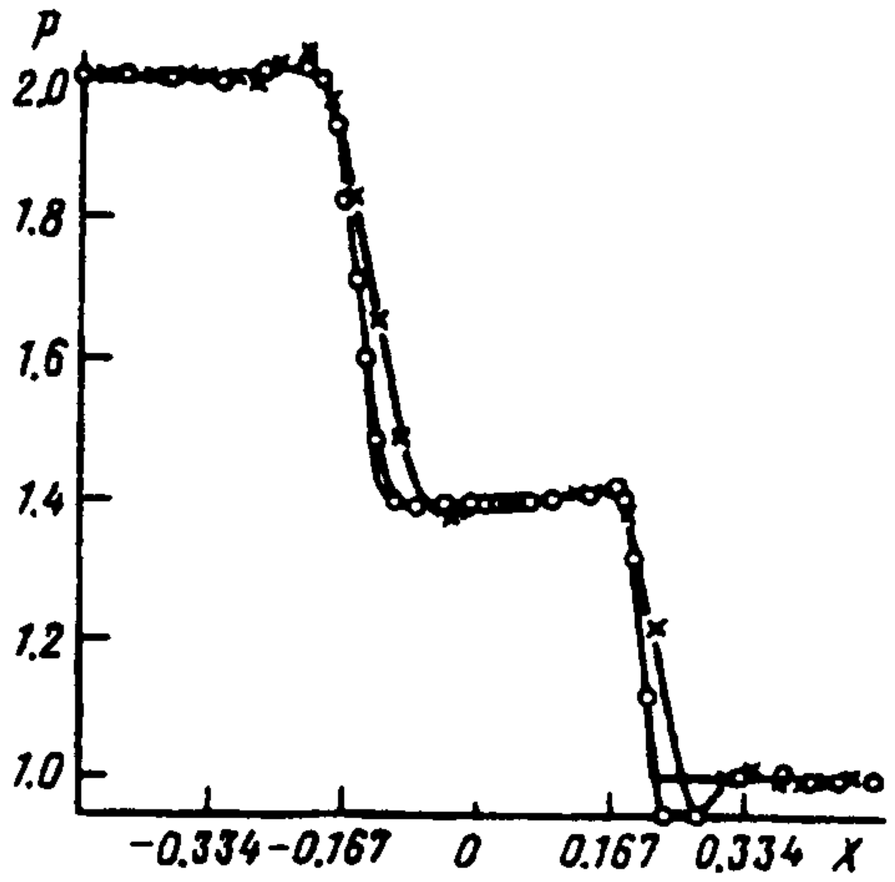

Fig. 4.

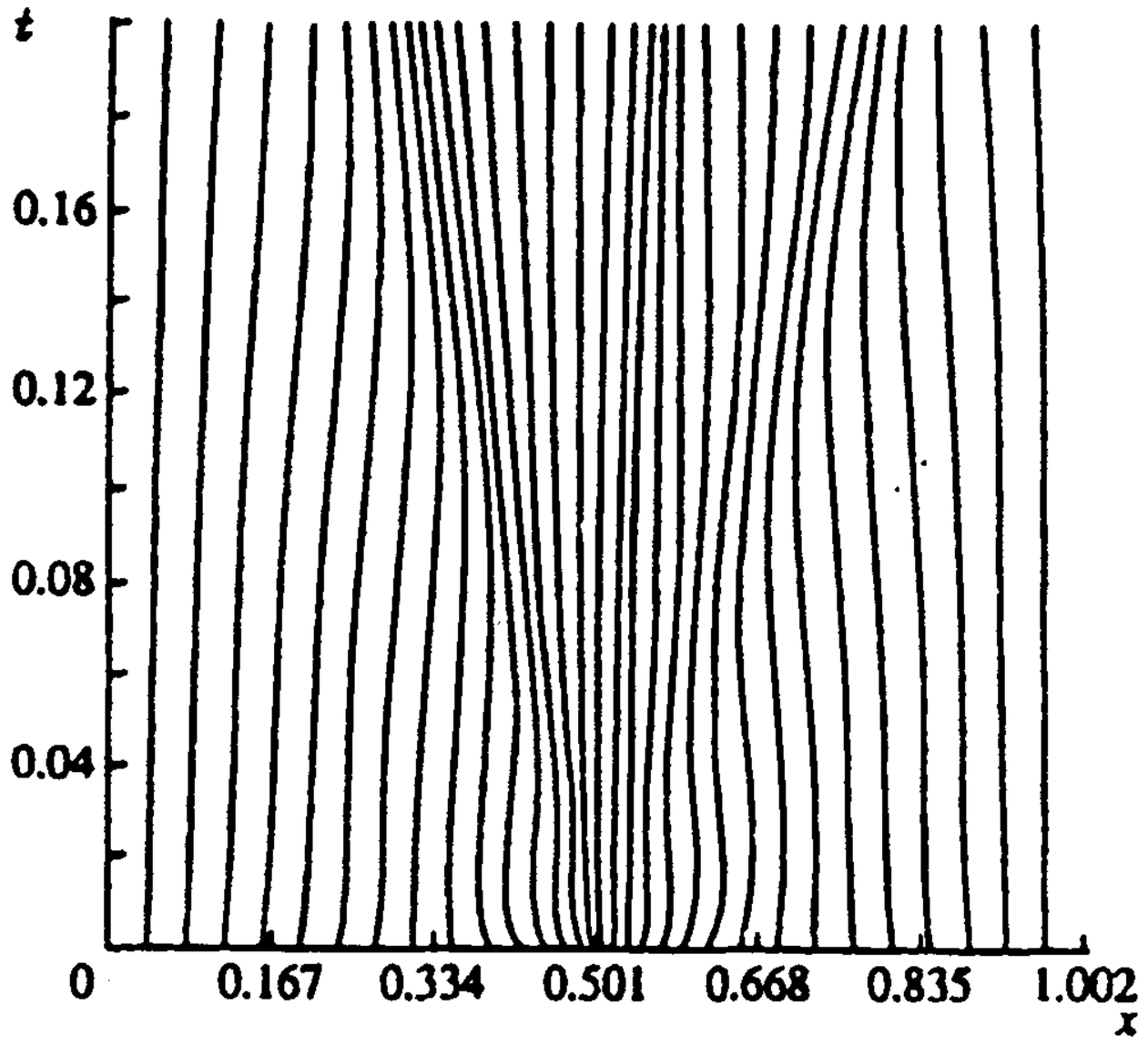

Fig. 5.

Here $\rho(x)$, $p(x)$ are the density and pressure, respectively.

Figure 1 shows the density distribution obtained on adaptive and uniform grids (with 16 nodes), as well as the analytic solution (the solid broken line). The distribution of the nodes of the uniform and adaptive grids for $t = 0.247$ is shown. Figure 2 shows the pressure distribution. It is clear from these results that the uniform grid does not have a sufficient number of nodes for the details of the solution to be resolved. However, the solution on the adaptive grid gives a well resolved rarefaction wave and contact discontinuity. The resolution on the shock wave is not quite as good. This is because there is only a small number of grid nodes in the neighbourhood of the shock wave.

Figures 3 and 4 show the same results for the adaptive and uniform grids for $t = 0.147$, but with a large number of nodes (32). The calculation on the adaptive grid is much more accurate than on the uniform grid with the same number of nodes.

Figure 5 shows the trajectories of the nodes of the adaptive grid. There are three regions where the nodes cluster, corresponding (from left to right) to the rarefaction wave, the contact discontinuity and the shock wave.

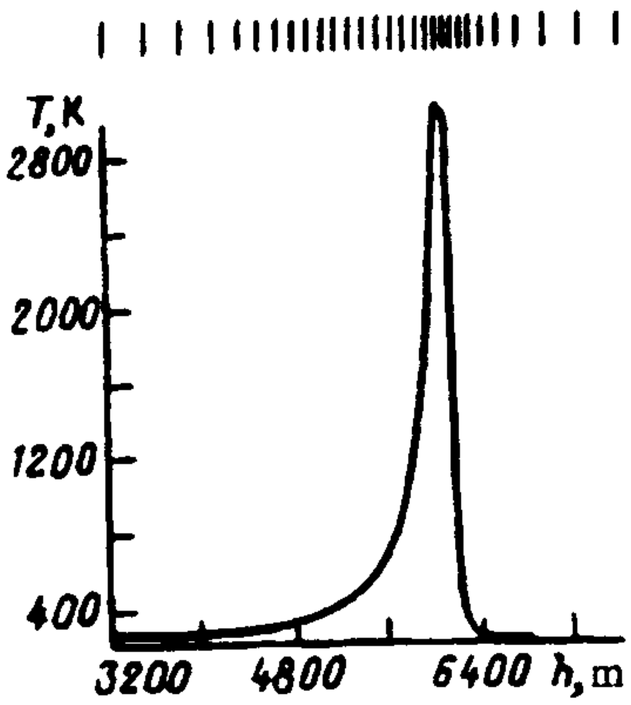

Fig. 6.

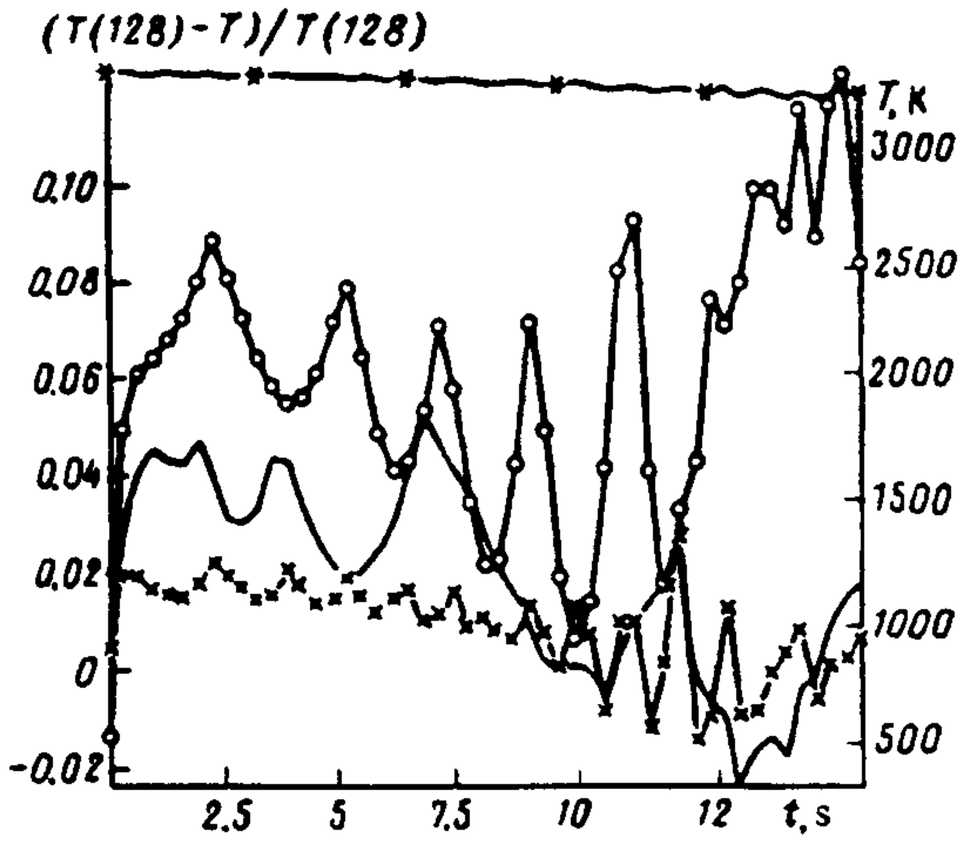

Fig. 7.

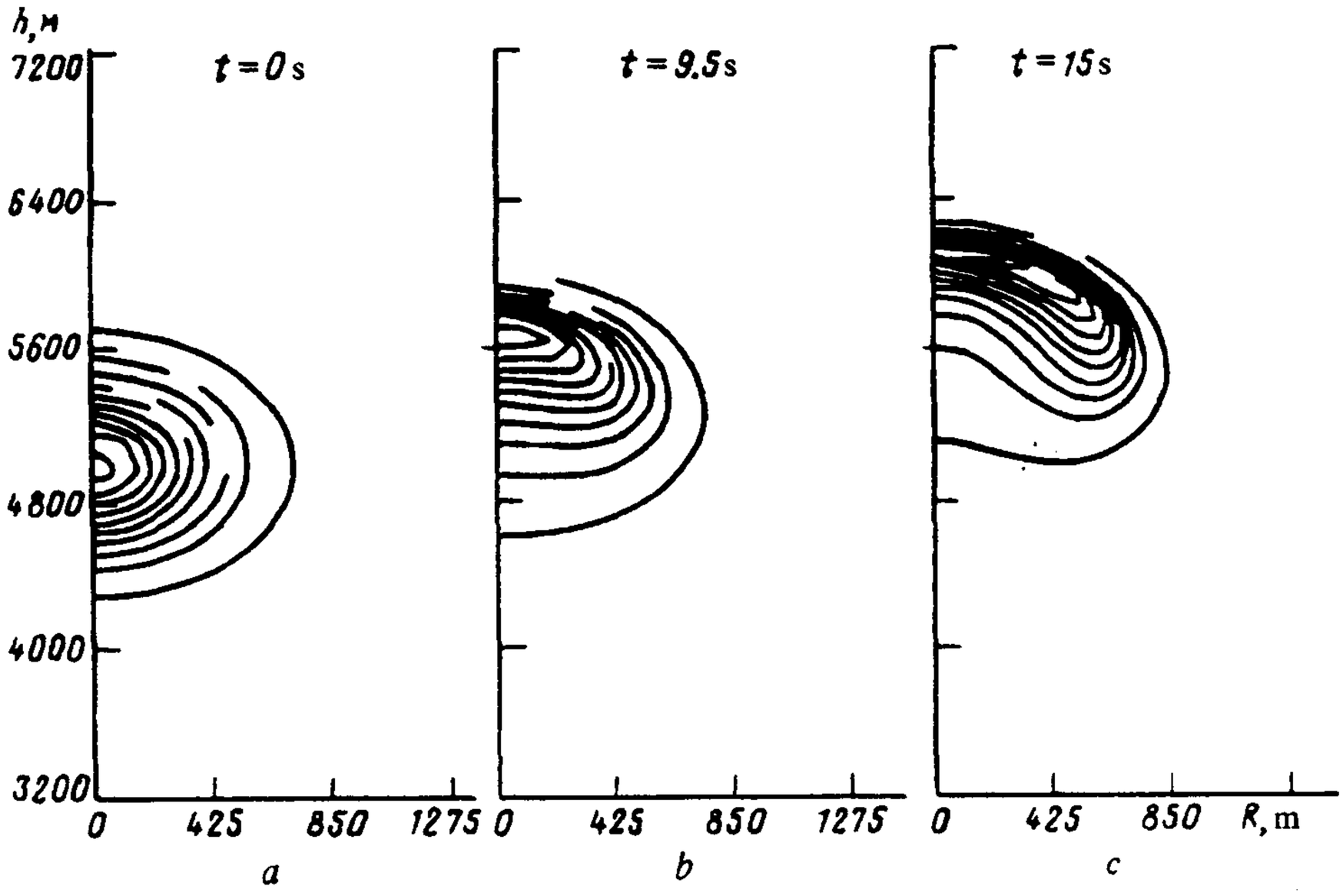

Fig. 8.

The second problem was two-dimensional. We considered the rising of a plane thermal in the stratified atmosphere of the earth. Because there was a plane of symmetry, we introduced a system of coordinates (z, r), where z is the distance from the earth's surface and r is the distance from the axis of symmetry. At the initial instant of time, the cloud of hot air is at rest. The temperature distribution has the form

$$T(z, r) = T_a(z, r) + T_s \exp\left[-\left(\frac{\alpha R}{R_s}\right)^2\right].$$

Here $T_a(z, r)$ is the temperature of the unperturbed atmosphere at a given point, $T_s = 3412$ K is the temperature increment above atmospheric temperature at the centre of the thermal, $R_s = 1325$ m is its radius, R is the distance from the centre of the thermal and $\alpha = 3.3$ is the constant of the exponential law.

The problem was simulated using Euler's equations. When the cloud surfaces, a vortical ring forms. The concentric temperature distribution distorts, forming a sharp temperature gradient on the upper edge of the cloud.

Figure 6 shows the temperature distribution in K on the line of symmetry at $t = 15$ s for an adaptive (32×16)-grid and the node distribution for z. The graph for the uniform (128×64) grid was almost the

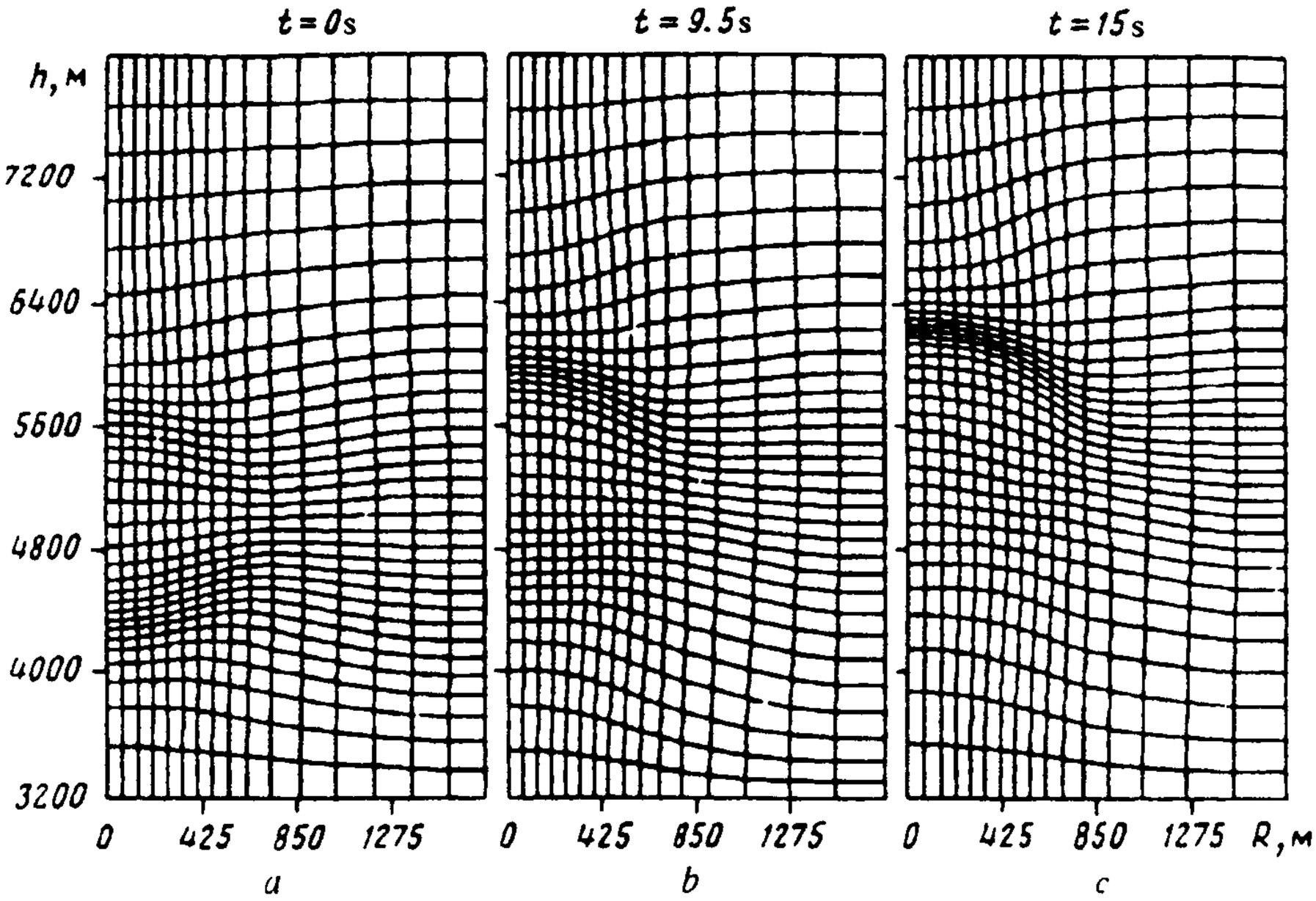

Fig. 9.

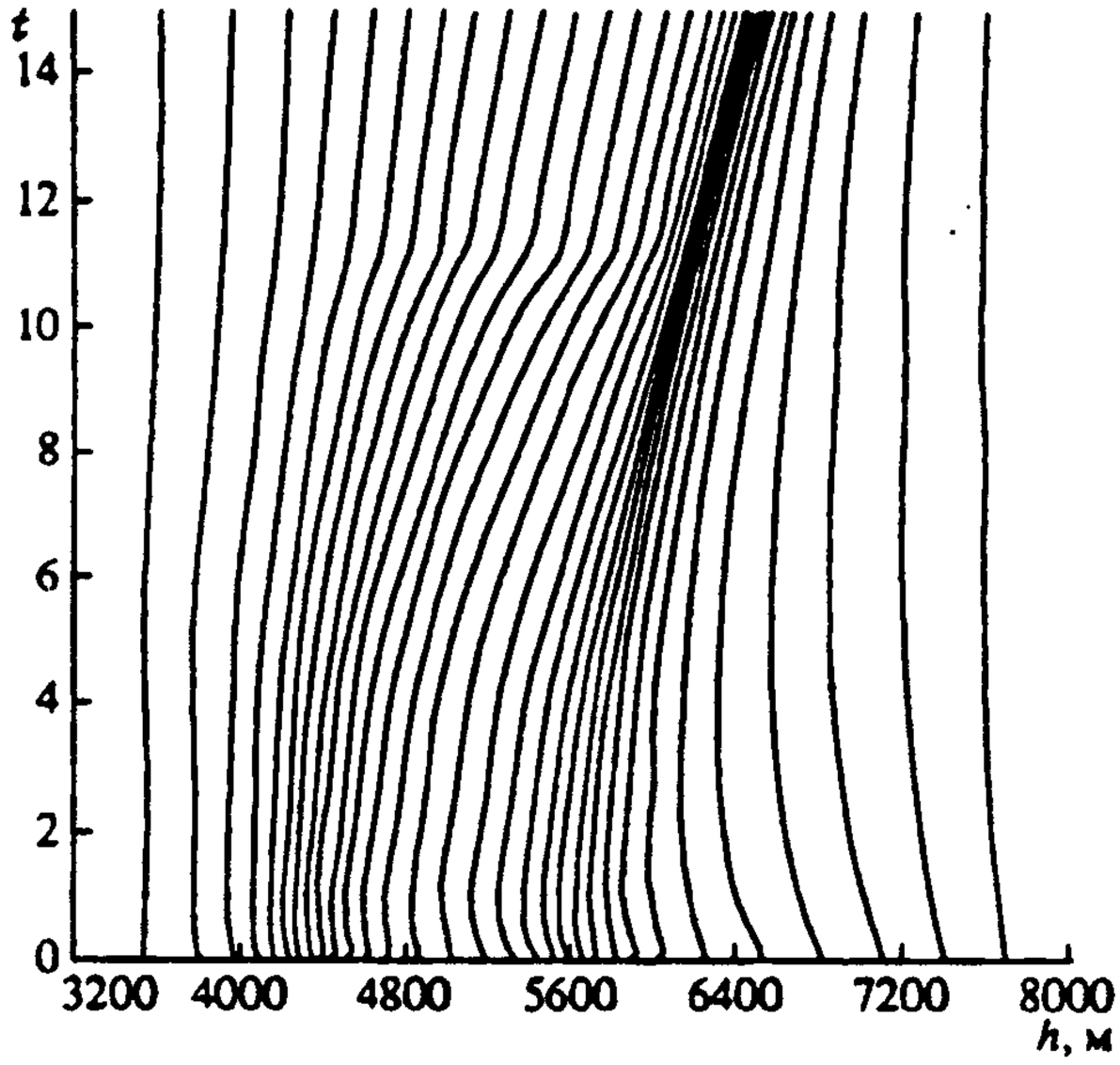

Fig. 10.

same as this distribution. There was a small difference in the case of a uniform (60 × 30) grid, for a uniform grid of the same size as the adaptive grid, the difference was more than 25%. Thus, a temperature gradient comparable to that obtained on the adaptive grid is achieved on a uniform grid with four times as many nodes in each direction. Figure 7 shows a graph of the maximum and calculation domains of temperature against time for a uniform grid (128 × 64, the marker is an asterisk) and the relative deviation from this distribution with an adaptive grid (32 × 16 — the solid curve) and a uniform grid (60 × 30 — the crosses and 32 × 16 — the small circles). This graph shows, first, convergence of the solution over the grid, and second, how close the solution on the adaptive grid is to the standard for this calculation.

Figure 8 shows the temperature contours in the calculation domain at different times. The calculation grids for the same times are shown in Fig. 9.

Figure 10 shows the trajectories of the grid nodes on the axis of symmetry. It can be seen that the grid follows the formation of a sharp temperature gradient on the upper edge of the cloud.

We wish to thank O. M. Belotserkovskii for his interest, and A. I. Tolstykh, with whom we had useful discussions.

REFERENCES

1. TOLSTYKH A. I., *Compact Difference Schemes and their Application in Fluid Dynamics*. Nauka, Moscow, 1990.
2. THOMAS P. D. and LOMBARD C. K., Geometric conservation law and its application to flow computations on moving grids. *AIAA Journal* **17**, 1030–1037, 1979.
3. OBAYASHI Sh., Freestream capturing for moving coordinates in three dimensions. *AIAA Journal* **30**, 1125–1128, 1992.
4. MUZAFAROV I. F. and UTYUZHNIKOV S. V., The application of compact difference schemes to the investigation of unsteady flows of a compressible gas. *Mat. Modelirovaniye* **5**, 74–83, 1992.
5. HINDMAN R. G. and SPENCER J., A new approach to truly adaptive grid generation. AIAA Paper, No. 83-0450.
6. YANENKO N. N., DANAYEV N. T. and LISEIKIN V. D., A variational method of grid construction. *Numerical Methods of the Mechanics of a Continuous Medium*. **8**, 4, 157–163. VTs SO Akad. Nauk S.S.S.R., Novosibirsk, 1977.
7. GAN'ZHA D. Kh. and UTYUZHNIKOV S. V., Some numerical methods of constructing solution-adaptive grids. *Applied Problems in Aeromechanics and Geospace Physics*, 68–83. MFTI, Moscow, 1993.